Cross Section Measurements of High-p_T Dilepton Final-State Processes Using a Global Fitting Method

A. Abulencia,[24] J. Adelman,[13] T. Affolder,[10] T. Akimoto,[56] M.G. Albrow,[17] D. Ambrose,[17] S. Amerio,[44] D. Amidei,[35] A. Anastassov,[53] K. Anikeev,[17] A. Annovi,[19] J. Antos,[14] M. Aoki,[56] G. Apollinari,[17] J.-F. Arguin,[34] T. Arisawa,[58] A. Artikov,[15] W. Ashmanskas,[17] A. Attal,[8] F. Azfar,[43] P. Azzi-Bacchetta,[44] P. Azzurri,[47] N. Bacchetta,[44] W. Badgett,[17] A. Barbaro-Galtieri,[29] V.E. Barnes,[49] B.A. Barnett,[25] S. Baroiant,[7] V. Bartsch,[31] G. Bauer,[33] F. Bedeschi,[47] S. Behari,[25] S. Belforte,[55] G. Bellettini,[47] J. Bellinger,[60] A. Belloni,[33] D. Benjamin,[16] A. Beretvas,[17] J. Beringer,[29] T. Berry,[30] A. Bhatti,[51] M. Binkley,[17] D. Bisello,[44] R.E. Blair,[2] C. Blocker,[6] B. Blumenfeld,[25] A. Bocci,[16] A. Bodek,[50] V. Boisvert,[50] G. Bolla,[49] A. Bolshov,[33] D. Bortoletto,[49] J. Boudreau,[48] A. Boveia,[10] B. Brau,[10] L. Brigliadori,[5] C. Bromberg,[36] E. Brubaker,[13] J. Budagov,[15] H.S. Budd,[50] S. Budd,[24] S. Budroni,[47] K. Burkett,[17] G. Busetto,[44] P. Bussey,[21] K. L. Byrum,[2] S. Cabrera[o],[16] M. Campanelli,[20] M. Campbell,[35] F. Canelli,[17] A. Canepa,[49] S. Carillo[i],[18] D. Carlsmith,[60] R. Carosi,[47] S. Carron,[34] M. Casarsa,[55] A. Castro,[5] P. Catastini,[47] D. Cauz,[55] M. Cavalli-Sforza,[3] A. Cerri,[29] L. Cerrito[m],[43] S.H. Chang,[28] Y.C. Chen,[1] M. Chertok,[7] G. Chiarelli,[47] G. Chlachidze,[15] F. Chlebana,[17] I. Cho,[28] K. Cho,[28] D. Chokheli,[15] J.P. Chou,[22] G. Choudalakis,[33] S.H. Chuang,[60] K. Chung,[12] W.H. Chung,[60] Y.S. Chung,[50] M. Ciljak,[47] C.I. Ciobanu,[24] M.A. Ciocci,[47] A. Clark,[20] D. Clark,[6] M. Coca,[16] G. Compostella,[44] M.E. Convery,[51] J. Conway,[7] B. Cooper,[36] K. Copic,[35] M. Cordelli,[19] G. Cortiana,[44] F. Crescioli,[47] C. Cuenca Almenar[o],[7] J. Cuevas[l],[11] R. Culbertson,[17] J.C. Cully,[35] D. Cyr,[60] S. DaRonco,[44] M. Datta,[17] S. D'Auria,[21] T. Davies,[21] M. D'Onofrio,[3] D. Dagenhart,[6] P. de Barbaro,[50] S. De Cecco,[52] A. Deisher,[29] G. De Lentdecker[c],[50] M. Dell'Orso,[47] F. Delli Paoli,[44] L. Demortier,[51] J. Deng,[16] M. Deninno,[5] D. De Pedis,[52] P.F. Derwent,[17] G.P. Di Giovanni,[45] C. Dionisi,[52] B. Di Ruzza,[55] J.R. Dittmann,[4] P. DiTuro,[53] C. Dörr,[26] S. Donati,[47] M. Donega,[20] P. Dong,[8] J. Donini,[44] T. Dorigo,[44] S. Dube,[53] J. Efron,[40] R. Erbacher,[7] D. Errede,[24] S. Errede,[24] R. Eusebi,[17] H.C. Fang,[29] S. Farrington,[30] I. Fedorko,[47] W.T. Fedorko,[13] R.G. Feild,[61] M. Feindt,[26] J.P. Fernandez,[32] R. Field,[18] G. Flanagan,[49] A. Foland,[22] S. Forrester,[7] G.W. Foster,[17] M. Franklin,[22] J.C. Freeman,[29] I. Furic,[13] M. Gallinaro,[51]

J. Galyardt,[12] J.E. Garcia,[47] F. Garberson,[10] A.F. Garfinkel,[49] C. Gay,[61] H. Gerberich,[24] D. Gerdes,[35] S. Giagu,[52] P. Giannetti,[47] A. Gibson,[29] K. Gibson,[48] J.L. Gimmell,[50] C. Ginsburg,[17] N. Giokaris[a],[15] M. Giordani,[55] P. Giromini,[19] M. Giunta,[47] G. Giurgiu,[12] V. Glagolev,[15] D. Glenzinski,[17] M. Gold,[38] N. Goldschmidt,[18] J. Goldstein[b],[43] A. Golossanov,[17] G. Gomez,[11] G. Gomez-Ceballos,[11] M. Goncharov,[54] O. González,[32] I. Gorelov,[38] A.T. Goshaw,[16] K. Goulianos,[51] A. Gresele,[44] M. Griffiths,[30] S. Grinstein,[22] C. Grosso-Pilcher,[13] R.C. Group,[18] U. Grundler,[24] J. Guimaraes da Costa,[22] Z. Gunay-Unalan,[36] C. Haber,[29] K. Hahn,[33] S.R. Hahn,[17] E. Halkiadakis,[53] A. Hamilton,[34] B.-Y. Han,[50] J.Y. Han,[50] R. Handler,[60] F. Happacher,[19] K. Hara,[56] M. Hare,[57] S. Harper,[43] R.F. Harr,[59] R.M. Harris,[17] M. Hartz,[48] K. Hatakeyama,[51] J. Hauser,[8] A. Heijboer,[46] B. Heinemann,[30] J. Heinrich,[46] C. Henderson,[33] M. Herndon,[60] J. Heuser,[26] D. Hidas,[16] C.S. Hill[b],[10] D. Hirschbuehl,[26] A. Hocker,[17] A. Holloway,[22] S. Hou,[1] M. Houlden,[30] S.-C. Hsu,[9] B.T. Huffman,[43] R.E. Hughes,[40] U. Husemann,[61] J. Huston,[36] J. Incandela,[10] G. Introzzi,[47] M. Iori,[52] Y. Ishizawa,[56] A. Ivanov,[7] B. Iyutin,[33] E. James,[17] D. Jang,[53] B. Jayatilaka,[35] D. Jeans,[52] H. Jensen,[17] E.J. Jeon,[28] S. Jindariani,[18] M. Jones,[49] K.K. Joo,[28] S.Y. Jun,[12] J.E. Jung,[28] T.R. Junk,[24] T. Kamon,[54] P.E. Karchin,[59] Y. Kato,[42] Y. Kemp,[26] R. Kephart,[17] U. Kerzel,[26] V. Khotilovich,[54] B. Kilminster,[40] D.H. Kim,[28] H.S. Kim,[28] J.E. Kim,[28] M.J. Kim,[12] S.B. Kim,[28] S.H. Kim,[56] Y.K. Kim,[13] N. Kimura,[56] L. Kirsch,[6] S. Klimenko,[18] M. Klute,[33] B. Knuteson,[33] B.R. Ko,[16] K. Kondo,[58] D.J. Kong,[28] J. Konigsberg,[18] A. Korytov,[18] A.V. Kotwal,[16] A. Kovalev,[46] A.C. Kraan,[46] J. Kraus,[24] I. Kravchenko,[33] M. Kreps,[26] J. Kroll,[46] N. Krumnack,[4] M. Kruse,[16] V. Krutelyov,[10] T. Kubo,[56] S. E. Kuhlmann,[2] T. Kuhr,[26] Y. Kusakabe,[58] S. Kwang,[13] A.T. Laasanen,[49] S. Lai,[34] S. Lami,[47] S. Lammel,[17] M. Lancaster,[31] R.L. Lander,[7] K. Lannon,[40] A. Lath,[53] G. Latino,[47] I. Lazzizzera,[44] T. LeCompte,[2] J. Lee,[50] J. Lee,[28] Y.J. Lee,[28] S.W. Lee[n],[54] R. Lefèvre,[3] N. Leonardo,[33] S. Leone,[47] S. Levy,[13] J.D. Lewis,[17] C. Lin,[61] C.S. Lin,[17] M. Lindgren,[17] E. Lipeles,[9] T.M. Liss,[24] A. Lister,[7] D.O. Litvintsev,[17] T. Liu,[17] N.S. Lockyer,[46] A. Loginov,[61] M. Loreti,[44] P. Loverre,[52] R.-S. Lu,[1] D. Lucchesi,[44] P. Lujan,[29] P. Lukens,[17] G. Lungu,[18] L. Lyons,[43] J. Lys,[29] R. Lysak,[14] E. Lytken,[49] P. Mack,[26] D. MacQueen,[34] R. Madrak,[17] K. Maeshima,[17] K. Makhoul,[33] T. Maki,[23] P. Maksimovic,[25] S. Malde,[43] G. Manca,[30] F. Margaroli,[5]

R. Marginean,[17] C. Marino,[26] C.P. Marino,[24] A. Martin,[61] M. Martin,[21] V. Martin[g],[21]
M. Martínez,[3] T. Maruyama,[56] P. Mastrandrea,[52] T. Masubuchi,[56] H. Matsunaga,[56]
M.E. Mattson,[59] R. Mazini,[34] P. Mazzanti,[5] K.S. McFarland,[50] P. McIntyre,[54]
R. McNulty[f],[30] A. Mehta,[30] P. Mehtala,[23] S. Menzemer[h],[11] A. Menzione,[47] P. Merkel,[49]
C. Mesropian,[51] A. Messina,[36] T. Miao,[17] N. Miladinovic,[6] J. Miles,[33] R. Miller,[36]
C. Mills,[10] M. Milnik,[26] A. Mitra,[1] G. Mitselmakher,[18] A. Miyamoto,[27] S. Moed,[20]
N. Moggi,[5] B. Mohr,[8] R. Moore,[17] M. Morello,[47] P. Movilla Fernandez,[29] J. Mülmenstädt,[29]
A. Mukherjee,[17] Th. Muller,[26] R. Mumford,[25] P. Murat,[17] J. Nachtman,[17] A. Nagano,[56]
J. Naganoma,[58] I. Nakano,[41] A. Napier,[57] V. Necula,[18] C. Neu,[46] M.S. Neubauer,[9]
J. Nielsen,[29] T. Nigmanov,[48] L. Nodulman,[2] O. Norniella,[3] E. Nurse,[31] S.H. Oh,[16]
Y.D. Oh,[28] I. Oksuzian,[18] T. Okusawa,[42] R. Oldeman,[30] R. Orava,[23] K. Osterberg,[23]
C. Pagliarone,[47] E. Palencia,[11] V. Papadimitriou,[17] A.A. Paramonov,[13] B. Parks,[40]
S. Pashapour,[34] J. Patrick,[17] G. Pauletta,[55] M. Paulini,[12] C. Paus,[33] D.E. Pellett,[7]
A. Penzo,[55] T.J. Phillips,[16] G. Piacentino,[47] J. Piedra,[45] L. Pinera,[18] K. Pitts,[24] C. Plager,[8]
L. Pondrom,[60] X. Portell,[3] O. Poukhov,[15] N. Pounder,[43] F. Prakoshyn,[15] A. Pronko,[17]
J. Proudfoot,[2] F. Ptohos[e],[19] G. Punzi,[47] J. Pursley,[25] J. Rademacker[b],[43] A. Rahaman,[48]
N. Ranjan,[49] S. Rappoccio,[22] B. Reisert,[17] V. Rekovic,[38] P. Renton,[43] M. Rescigno,[52]
S. Richter,[26] F. Rimondi,[5] L. Ristori,[47] A. Robson,[21] T. Rodrigo,[11] E. Rogers,[24]
S. Rolli,[57] R. Roser,[17] M. Rossi,[55] R. Rossin,[18] A. Ruiz,[11] J. Russ,[12] V. Rusu,[13]
H. Saarikko,[23] S. Sabik,[34] A. Safonov,[54] W.K. Sakumoto,[50] G. Salamanna,[52] O. Saltó,[3]
D. Saltzberg,[8] C. Sánchez,[3] L. Santi,[55] S. Sarkar,[52] L. Sartori,[47] K. Sato,[17] P. Savard,[34]
A. Savoy-Navarro,[45] T. Scheidle,[26] P. Schlabach,[17] E.E. Schmidt,[17] M.P. Schmidt,[61]
M. Schmitt,[39] T. Schwarz,[7] L. Scodellaro,[11] A.L. Scott,[10] A. Scribano,[47] F. Scuri,[47]
A. Sedov,[49] S. Seidel,[38] Y. Seiya,[42] A. Semenov,[15] L. Sexton-Kennedy,[17] A. Sfyrla,[20]
M.D. Shapiro,[29] T. Shears,[30] P.F. Shepard,[48] D. Sherman,[22] M. Shimojima[k],[56]
M. Shochet,[13] Y. Shon,[60] I. Shreyber,[37] A. Sidoti,[47] P. Sinervo,[34] A. Sisakyan,[15]
J. Sjolin,[43] A.J. Slaughter,[17] J. Slaunwhite,[40] K. Sliwa,[57] J.R. Smith,[7] F.D. Snider,[17]
R. Snihur,[34] M. Soderberg,[35] A. Soha,[7] S. Somalwar,[53] V. Sorin,[36] J. Spalding,[17]
F. Spinella,[47] T. Spreitzer,[34] P. Squillacioti,[47] M. Stanitzki,[61] A. Staveris-Polykalas,[47]
R. St. Denis,[21] B. Stelzer,[8] O. Stelzer-Chilton,[43] D. Stentz,[39] J. Strologas,[38] D. Stuart,[10]

J.S. Suh,[28] A. Sukhanov,[18] H. Sun,[57] T. Suzuki,[56] A. Taffard,[24] R. Takashima,[41] Y. Takeuchi,[56] K. Takikawa,[56] M. Tanaka,[2] R. Tanaka,[41] M. Tecchio,[35] P.K. Teng,[1] K. Terashi,[51] J. Thom[d],[17] A.S. Thompson,[21] E. Thomson,[46] P. Tipton,[61] V. Tiwari,[12] S. Tkaczyk,[17] D. Toback,[54] S. Tokar,[14] K. Tollefson,[36] T. Tomura,[56] D. Tonelli,[47] S. Torre,[19] D. Torretta,[17] S. Tourneur,[45] W. Trischuk,[34] R. Tsuchiya,[58] S. Tsuno,[41] N. Turini,[47] F. Ukegawa,[56] T. Unverhau,[21] S. Uozumi,[56] D. Usynin,[46] S. Vallecorsa,[20] N. van Remortel,[23] A. Varganov,[35] E. Vataga,[38] F. Vázquez[i],[18] G. Velev,[17] G. Veramendi,[24] V. Veszpremi,[49] R. Vidal,[17] I. Vila,[11] R. Vilar,[11] T. Vine,[31] I. Vollrath,[34] I. Volobouev[n],[29] G. Volpi,[47] F. Würthwein,[9] P. Wagner,[54] R.G. Wagner,[2] R.L. Wagner,[17] J. Wagner,[26] W. Wagner,[26] R. Wallny,[8] S.M. Wang,[1] A. Warburton,[34] S. Waschke,[21] D. Waters,[31] M. Weinberger,[54] W.C. Wester III,[17] B. Whitehouse,[57] D. Whiteson,[46] A.B. Wicklund,[2] E. Wicklund,[17] G. Williams,[34] H.H. Williams,[46] P. Wilson,[17] B.L. Winer,[40] P. Wittich[d],[17] S. Wolbers,[17] C. Wolfe,[13] T. Wright,[35] X. Wu,[20] S.M. Wynne,[30] A. Yagil,[17] K. Yamamoto,[42] J. Yamaoka,[53] T. Yamashita,[41] C. Yang,[61] U.K. Yang[j],[13] Y.C. Yang,[28] W.M. Yao,[29] G.P. Yeh,[17] J. Yoh,[17] K. Yorita,[13] T. Yoshida,[42] G.B. Yu,[50] I. Yu,[28] S.S. Yu,[17] J.C. Yun,[17] L. Zanello,[52] A. Zanetti,[55] I. Zaw,[22] X. Zhang,[24] J. Zhou,[53] and S. Zucchelli[5]

(CDF Collaboration*)

[1]*Institute of Physics, Academia Sinica, Taipei, Taiwan 11529, Republic of China*

[2]*Argonne National Laboratory, Argonne, Illinois 60439*

[3]*Institut de Fisica d'Altes Energies, Universitat Autonoma de Barcelona, E-08193, Bellaterra (Barcelona), Spain*

[4]*Baylor University, Waco, Texas 76798*

[5]*Istituto Nazionale di Fisica Nucleare, University of Bologna, I-40127 Bologna, Italy*

* With visitors from [a]University of Athens, [b]University of Bristol, [c]University Libre de Bruxelles, [d]Cornell University, [e]University of Cyprus, [f]University of Dublin, [g]University of Edinburgh, [h]University of Heidelberg, [i]Universidad Iberoamericana, [j]University of Manchester, [k]Nagasaki Institute of Applied Science, [l]University de Oviedo, [m]University of London, Queen Mary and Westfield College, [n]Texas Tech University, [o]IFIC(CSIC-Universitat de Valencia),

[6]*Brandeis University, Waltham, Massachusetts 02254*

[7]*University of California, Davis, Davis, California 95616*

[8]*University of California, Los Angeles, Los Angeles, California 90024*

[9]*University of California, San Diego, La Jolla, California 92093*

[10]*University of California, Santa Barbara, Santa Barbara, California 93106*

[11]*Instituto de Fisica de Cantabria, CSIC-University of Cantabria, 39005 Santander, Spain*

[12]*Carnegie Mellon University, Pittsburgh, PA 15213*

[13]*Enrico Fermi Institute, University of Chicago, Chicago, Illinois 60637*

[14]*Comenius University, 842 48 Bratislava,*
Slovakia; Institute of Experimental Physics, 040 01 Kosice, Slovakia

[15]*Joint Institute for Nuclear Research, RU-141980 Dubna, Russia*

[16]*Duke University, Durham, North Carolina 27708*

[17]*Fermi National Accelerator Laboratory, Batavia, Illinois 60510*

[18]*University of Florida, Gainesville, Florida 32611*

[19]*Laboratori Nazionali di Frascati, Istituto Nazionale*
di Fisica Nucleare, I-00044 Frascati, Italy

[20]*University of Geneva, CH-1211 Geneva 4, Switzerland*

[21]*Glasgow University, Glasgow G12 8QQ, United Kingdom*

[22]*Harvard University, Cambridge, Massachusetts 02138*

[23]*Division of High Energy Physics, Department of Physics,*
University of Helsinki and Helsinki Institute of Physics, FIN-00014, Helsinki, Finland

[24]*University of Illinois, Urbana, Illinois 61801*

[25]*The Johns Hopkins University, Baltimore, Maryland 21218*

[26]*Institut für Experimentelle Kernphysik,*
Universität Karlsruhe, 76128 Karlsruhe, Germany

[27]*High Energy Accelerator Research Organization (KEK), Tsukuba, Ibaraki 305, Japan*

[28]*Center for High Energy Physics: Kyungpook National University,*
Taegu 702-701, Korea; Seoul National University, Seoul 151-742,
Korea; and SungKyunKwan University, Suwon 440-746, Korea

[29]*Ernest Orlando Lawrence Berkeley National Laboratory, Berkeley, California 94720*

[30]*University of Liverpool, Liverpool L69 7ZE, United Kingdom*

[31]*University College London, London WC1E 6BT, United Kingdom*

[32]*Centro de Investigaciones Energeticas Medioambientales y Tecnologicas, E-28040 Madrid, Spain*

[33]*Massachusetts Institute of Technology, Cambridge, Massachusetts 02139*

[34]*Institute of Particle Physics: McGill University, Montréal, Canada H3A 2T8; and University of Toronto, Toronto, Canada M5S 1A7*

[35]*University of Michigan, Ann Arbor, Michigan 48109*

[36]*Michigan State University, East Lansing, Michigan 48824*

[37]*Institution for Theoretical and Experimental Physics, ITEP, Moscow 117259, Russia*

[38]*University of New Mexico, Albuquerque, New Mexico 87131*

[39]*Northwestern University, Evanston, Illinois 60208*

[40]*The Ohio State University, Columbus, Ohio 43210*

[41]*Okayama University, Okayama 700-8530, Japan*

[42]*Osaka City University, Osaka 588, Japan*

[43]*University of Oxford, Oxford OX1 3RH, United Kingdom*

[44]*University of Padova, Istituto Nazionale di Fisica Nucleare, Sezione di Padova-Trento, I-35131 Padova, Italy*

[45]*LPNHE, Universite Pierre et Marie Curie/IN2P3-CNRS, UMR7585, Paris, F-75252 France*

[46]*University of Pennsylvania, Philadelphia, Pennsylvania 19104*

[47]*Istituto Nazionale di Fisica Nucleare Pisa, Universities of Pisa, Siena and Scuola Normale Superiore, I-56127 Pisa, Italy*

[48]*University of Pittsburgh, Pittsburgh, Pennsylvania 15260*

[49]*Purdue University, West Lafayette, Indiana 47907*

[50]*University of Rochester, Rochester, New York 14627*

[51]*The Rockefeller University, New York, New York 10021*

[52]*Istituto Nazionale di Fisica Nucleare, Sezione di Roma 1, University of Rome "La Sapienza," I-00185 Roma, Italy*

[53]*Rutgers University, Piscataway, New Jersey 08855*

[54]*Texas A&M University, College Station, Texas 77843*

[55]*Istituto Nazionale di Fisica Nucleare, University of Trieste/ Udine, Italy*

[56]*University of Tsukuba, Tsukuba, Ibaraki 305, Japan*

[57]*Tufts University, Medford, Massachusetts 02155*

[58] *Waseda University, Tokyo 169, Japan*
[59] *Wayne State University, Detroit, Michigan 48201*
[60] *University of Wisconsin, Madison, Wisconsin 53706*
[61] *Yale University, New Haven, Connecticut 06520*

(Dated: December 22, 2006)

Abstract

We present a new method for studying high-p_T dilepton events ($e^{\pm}e^{\mp}$, $\mu^{\pm}\mu^{\mp}$, $e^{\pm}\mu^{\mp}$) and simultaneously extracting the production cross sections of $p\bar{p} \to t\bar{t}$, $p\bar{p} \to W^+W^-$, and $p\bar{p} \to Z^0 \to \tau^+\tau^-$ at a center-of-mass energy of $\sqrt{s} = 1.96\,\mathrm{TeV}$. We perform a likelihood fit to the dilepton data in a parameter space defined by the missing transverse energy and the number of jets in the event. Our results, which use $360\,\mathrm{pb}^{-1}$ of data recorded with the CDF II detector at the Fermilab Tevatron Collider, are $\sigma(t\bar{t}) = 8.5^{+2.7}_{-2.2}\,\mathrm{pb}$, $\sigma(W^+W^-) = 16.3^{+5.2}_{-4.4}\,\mathrm{pb}$, and $\sigma(Z^0 \to \tau^+\tau^-) = 291^{+50}_{-46}\,\mathrm{pb}$.

PACS numbers: 14.70.-e, 13.85.Qk, 13.85.Ni

There are relatively few standard model (SM) processes that contribute significantly to a final-state containing a pair of highly energetic charged leptons. The processes that can contribute to these "dilepton" events include top-quark pair ($t\bar{t}$) production, W-boson pair (W^+W^-) production, and Drell-Yan processes. The distinctiveness of this final-state offers unique tests of the SM and an intriguing potential for revealing new physics. For instance, in Run I (1992-1996) the Collider Detector at Fermilab (CDF) observed several $t\bar{t}$ candidate events in the dilepton decay mode [1] with unusual characteristics, and it was suggested that the kinematics of these events could be better described by the cascade decays of heavy supersymmetric quarks [2]. Furthermore, the top-quark's extraordinarily large mass might be an indication of a close connection with the mechanism of mass generation itself, as for example, in the model of topcolor assisted technicolor [3], which predicts new resonances decaying to $t\bar{t}$. In addition, a fourth generation fermion family [4] could enhance the gluon-gluon fusion Higgs production cross section by an order of magnitude, which, for a heavy Higgs boson, would lead to an increase in the number of W boson pairs observed [5]. These examples could all produce an excess of dilepton events in our data, which, depending on the topology of the new physics, would affect the cross section measurements of the main SM processes to different extents. This provides the motivation behind the present study of highly energetic dilepton events.

The main SM processes with a high-p_T [6] dilepton final-state can be identified based on their distinct event characteristics. For example, $t\bar{t}$ and W^+W^- production with decays in the $e\mu$ dilepton channel, $t\bar{t} \to W^+ b\, W^- \bar{b} \to e^{\pm}\mu^{\mp}\, \nu\bar{\nu}\, b\bar{b}$ and $W^+W^- \to e^{\pm}\mu^{\mp}\, \nu\bar{\nu}$, and the di-tau decays of Z^0 bosons, $Z^0 \to \tau^+\tau^- \to e^{\pm}\mu^{\mp}\nu\nu\bar{\nu}\bar{\nu}$, can be distinguished from each other by the number of jets, N_j, and the missing transverse energy [7], $\not\!\!E_T$, in the event. Both $t\bar{t}$ and W^+W^- events typically have large $\not\!\!E_T$ from the final-state undetected neutrinos; however, due to the two final state b-quarks, $t\bar{t}$ has a greater number of jets than W^+W^-. Conversely, $Z^0 \to \tau^+\tau^-$ events have small $\not\!\!E_T$ (due to the neutrinos being of lower energy than in the $t\bar{t}$ and W^+W^- processes, and typically traveling in opposite directions), and most often no jets. For both W^+W^- and $Z^0 \to \tau^+\tau^-$ events, jets can arise only through higher-order processes that include initial-state gluon radiation.

In contrast to analyses dedicated to measuring a single SM process, the analysis presented here adopts a more global strategy by considering all events with a high-p_T electron and muon, and making no further selection requirements. We then exploit the different $\not\!\!E_T$ and

N_j characteristics to simultaneously extract the production cross sections of the three main processes described. This is done by fitting the $e\mu$ data in a two-dimensional (2-D) $\not\!\!E_T - N_j$ parameter space to template distributions of $t\bar{t}$, W^+W^-, and $Z^0 \to \tau^+\tau^-$ events. Less significant processes are also taken into account.

We also consider the ee and $\mu\mu$ final-states, in addition to $e\mu$, but in these cases we have the added complication of a large Drell-Yan ($Z^0/\gamma^* \to e^+e^-$ or $\mu^+\mu^-$) contribution, necessitating a different treatment for these channels. This involves reducing the Drell-Yan ee and $\mu\mu$ contributions by requiring events to have significant $\not\!\!E_T$ in those channels. Without this requirement the $t\bar{t}$ and W^+W^- contributions to the ee and $\mu\mu$ events would be overwhelmed, rendering these final-states unusable. Our $t\bar{t}$ and W^+W^- results use all three dilepton final-states. For extracting the $Z^0 \to \tau^+\tau^-$ cross section we use only $e\mu$ events as the removal of Drell-Yan ee and $\mu\mu$ events also significantly reduces the $Z^0 \to \tau^+\tau^-$ contribution in the ee and $\mu\mu$ channels.

Since this method makes minimal requirements on events after requiring two leptons, it utilizes the full statistical power of the data for given lepton definitions. In the present analysis we have chosen to use very tight lepton identification requirements to demonstrate the method, and establish a foundation for future measurements with more data. This gives us greater control of the background processes, in particular those involving jets being misidentified as, or containing, leptons. However, it also reduces the potential statistical gain from the method. Even so, the results are comparable in precision to the analyses dedicated to the individual cross section measurements, and that use looser dilepton definitions. Furthermore, by looking at all processes simultaneously in the same generic dilepton sample, this method tests the SM consistency in a way an analysis dedicated to a single cross section measurement does not. An additional benefit of minimizing the requirements on the event after two high-p_T leptons are selected is the possibility for sensitivity to new physics which might fall into the $\not\!\!E_T - N_j$ parameter space that we study.

The data sample was collected with the CDF II detector between 2002 and 2004, and corresponds to an integrated luminosity of approximately 360 pb^{-1}. The results presented here complement the individual cross section measurements from CDF for each process [8–10], which make additional requirements to reduce, and assume the SM cross sections for all the processes in the dilepton sample other than the one being measured.

The CDF II detector has a general-purpose design [11]. The components relevant to

this analysis are briefly described here. A tracking system inside a 1.4 T superconducting solenoidal magnet is composed of silicon detectors for high-precision track measurements, and an open-cell drift chamber surrounding the silicon system. Electromagnetic and hadronic calorimeters surround the tracking system and solenoid and are used to measure the energy of interacting particles. In this analysis information is used from both the central (covering the pseudo-rapidity range $|\eta| < 1.1$) and end-plug detectors (of which we use the range $1.2 < |\eta| < 2.0$) to identify electron candidates. The missing transverse energy calculation uses calorimeter towers with $|\eta| < 3.5$. We identify jets using clusters of calorimeter towers above an energy threshold of 3 GeV, with fixed cone radius $\Delta R = \sqrt{\Delta\phi^2 + \Delta\eta^2} = 0.4$. The jet transverse energy is corrected for the calorimeter response and multiple interactions [12, 13]. We require that the corrected jets have $E_T > 15$ GeV and $|\eta| < 2.5$. A set of drift chambers located outside the central hadronic calorimeters are used to detect muons in the region $|\eta| < 0.6$. Additional drift chambers and scintillation counters detect muons in the region $0.6 < |\eta| < 1.0$.

A three-level trigger system is used to select events. The triggers employed to collect events for this analysis are [14] an inclusive central electron ($|\eta| < 1.1$) trigger requiring an electron with $E_T > 18$ GeV, and an inclusive central muon ($|\eta| < 1.0$) trigger requiring a muon with $p_T > 18$ GeV/c.

Events selected for the analysis contain two opposite sign leptons (electrons or muons) consistent with originating from the same vertex, and with $E_T > 20$ GeV for electrons and $p_T > 20$ GeV/c for muons. Muons from cosmic rays and electrons from photon conversions are removed, as described in Ref. [14]. Both leptons are required to be isolated in the calorimeter [15] and the tracking chamber [16], in order to reduce the probability that a jet is misidentified as a lepton, or that a selected lepton comes from the semileptonic decay of b or c hadrons.

We consider three classes of dilepton events: $e\mu$, ee, and $\mu\mu$. For the $e\mu$ channel we make no further requirements on the event after the selection of two leptons as described above, and simply count the number of jets, N_j, and measure the $\not\!\!E_T$ in the event.

The ee and $\mu\mu$ channels have a large Drell-Yan contribution which we reduce significantly by applying a requirement on the missing transverse energy significance defined by:

$$\not\!\!E_T^{sig} = \frac{\not\!\!E_T}{\sqrt{\sum E_T}}$$

where $\sum E_T$ is the sum of transverse energies over all calorimeter towers, corrected to include the p_T of the muons. We require $\not\!\!E_T^{sig} > 2.5\,\mathrm{GeV}^{1/2}$ for all ee and $\mu\mu$ events .

After the above dilepton and $\not\!\!E_T^{sig}$ requirements, the dominant SM contributions which we consider as our signal processes, are $t\bar{t} \to W^+ b\, W^- \bar{b} \to \ell^+ \nu b\, \ell^- \bar{\nu} \bar{b}$, $W^+W^- \to \ell^+ \nu\, \ell^- \bar{\nu}$, and $Z^0 \to \tau^+\tau^- \to \ell^+ \nu_\ell \bar{\nu}_\tau\, \ell^- \bar{\nu}_\ell \nu_\tau$, where ℓ indicates an electron or muon. These processes are separated in our chosen $\not\!\!E_T - N_j$ parameter space as previously explained. The predicted distributions of these signal processes in the $\not\!\!E_T - N_j$ parameter space for the $e\mu$ channel are shown in Fig. 1, and were obtained from Monte Carlo simulations.

Contributions to the dilepton sample which we consider as background processes, include Drell-Yan (ee, $\mu\mu$), WZ, ZZ, $W + \gamma$, and $W +$ jets. Note that Drell-Yan $\mu\mu$ events could be reconstructed as an $e\mu$ final-state when a muon in the forward region radiates a photon that is misidentified as an electron. The predicted combined background distributions in the $\not\!\!E_T - N_j$ parameter space is also shown in Fig. 1. We fit the data $e\mu$, ee, and $\mu\mu$ distributions to the expected signal shapes, letting each of their normalizations float in the fit. The $e\mu$ data distribution is shown in Fig. 2, of which about 60% of the events are expected to be from $Z^0 \to \tau^+\tau^-$ and concentrated in the low-$\not\!\!E_T$, zero-jet region of the $\not\!\!E_T - N_j$ parameter space.

To determine the acceptance of our selection criteria for the $t\bar{t}$, W^+W^-, and $Z^0 \to \tau^+\tau^-$ processes we use the PYTHIA [17] Monte Carlo program, followed by a full simulation of the CDF II detector which is based on the GEANT simulation program [18]. The acceptances for each of these processes are shown in Table I. The $Z^0 \to \tau^+\tau^-$ acceptances are defined as the fraction of $Z^0/\gamma^* \to \tau^+\tau^-$ events generated in the di-tau mass range of $66 < M_{\tau\tau} < 116\,\mathrm{GeV}/c^2$ that pass our dilepton selection criteria. The contribution from γ^* is only about 0.3%. For the ee and $\mu\mu$ channels the additional $\not\!\!E_T^{sig}$ requirement removes 32% of $t\bar{t}$ events and 36% of W^+W^- events, while also removing about 99.8% of Drell-Yan events.

The systematic uncertainties on the $t\bar{t}$, W^+W^-, and $Z^0 \to \tau^+\tau^-$ acceptances, summarized in Table II, result from uncertainties in the jet energy scale (JES) [13], the modeling of the initial-state radiation (ISR) by PYTHIA [and for the case of $t\bar{t}$ also final-state radiation (FSR)], the uncertainty on the parton distribution functions [19], the modeling of $\not\!\!E_T^{sig}$, and uncertainties in the lepton trigger and identification efficiencies. The $\not\!\!E_T^{sig}$ systematic uncertainty does not apply to the $Z^0 \to \tau^+\tau^-$ cross section measurement, as we fit for this only in the $e\mu$ channel. Moreover, the $e\mu$ channel acceptance does not suffer from a jet

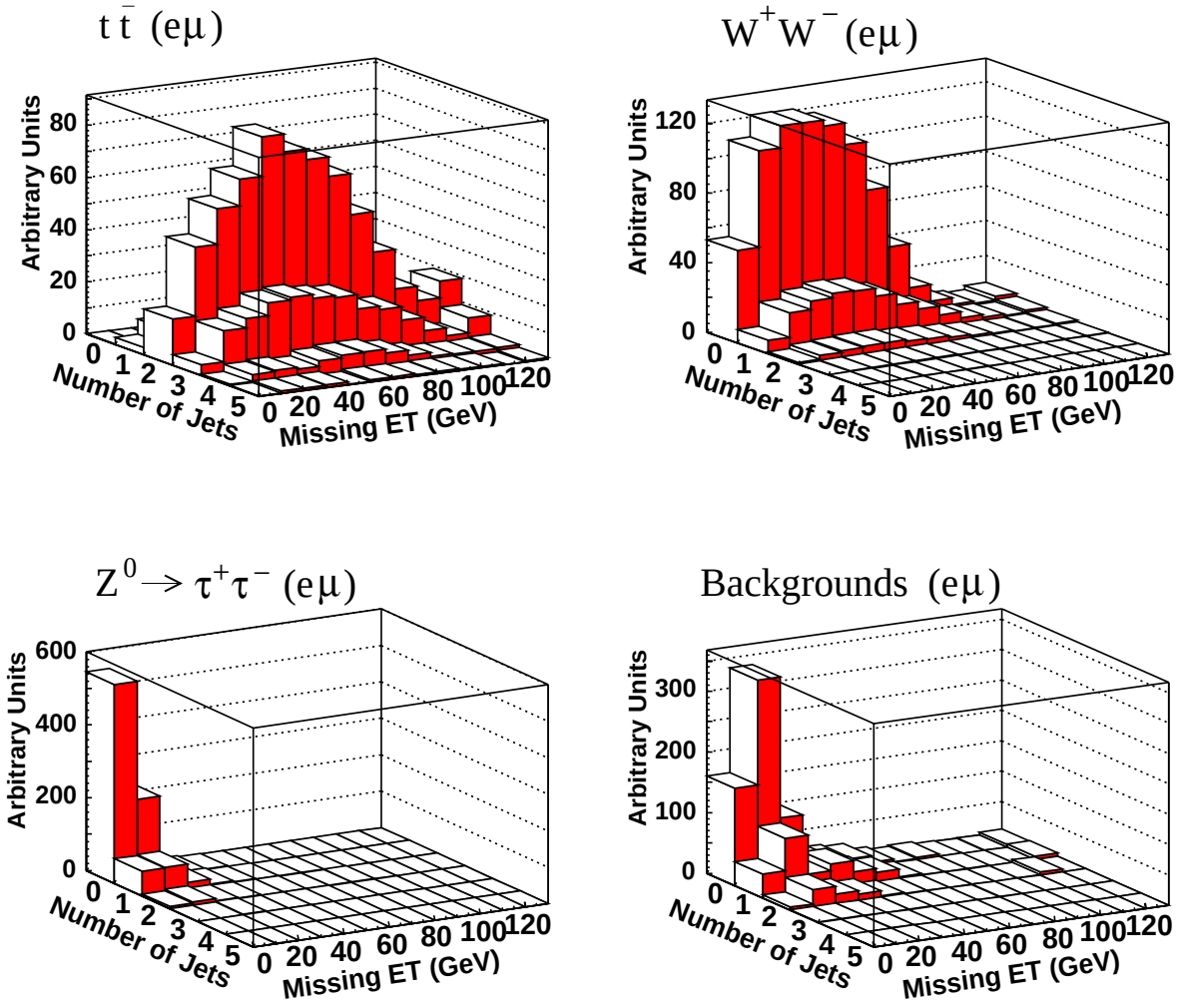

FIG. 1: The $\not\!\!E_T - N_j$ distributions for $t\bar{t}$, W^+W^-, $Z^0 \to \tau^+\tau^-$ in the $e\mu$ channel. Also shown is the combined background distribution for the $e\mu$ channel. All the distributions are normalized to an arbitrary equal volume. The numbers of events expected in $360\,\mathrm{pb}^{-1}$ for each source are given in Table III. The highest $\not\!\!E_T$ and N_j bins include any overflow events.

energy scale uncertainty, as we include $e\mu$ events with all jet multiplicities, whereas for the ee and $\mu\mu$ channels this systematic uncertainty enters through the $\not\!\!E_T^{sig}$ requirement. A 6% uncertainty on the integrated luminosity is applied to the expected number of events for all processes [22].

The Drell-Yan and diboson (WZ, ZZ) backgrounds are determined using PYTHIA Monte Carlo, followed by the detector simulation. We normalize the total number of events for these

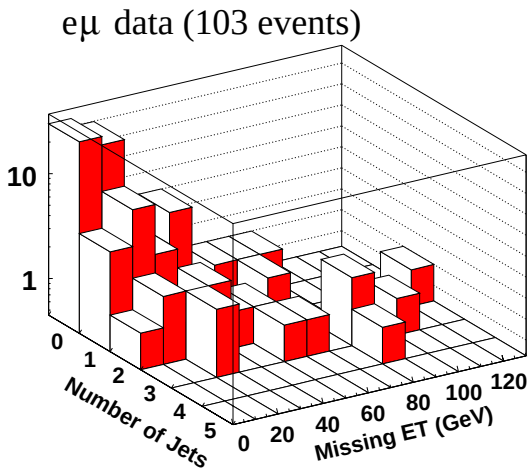

FIG. 2: The $\not\!\!E_T - N_j$ distribution for data in the $e\mu$ channel. The log scale is used to make the low count bins more visible.

TABLE I: Summary of acceptances for $t\bar{t}$, W^+W^-, and $Z^0 \to \tau^+\tau^-$ events, where the quoted errors include the systematic uncertainties from Table II. Values include SM branching fractions to the dilepton final-state. The $t\bar{t}$ events were simulated with a top quark mass of 178 GeV/c^2.

	$e\mu$	ee	$\mu\mu$
$t\bar{t}$	$(0.399 \pm 0.029)\%$	$(0.144 \pm 0.019)\%$	$(0.136 \pm 0.015)\%$
W^+W^-	$(0.294 \pm 0.018)\%$	$(0.111 \pm 0.008)\%$	$(0.092 \pm 0.006)\%$
$Z \to \tau\tau$	$(0.0458 \pm 0.0032)\%$	$(0.0008 \pm 0.0001)\%$	$(0.0005 \pm 0.0001)\%$

processes to theoretical cross section predictions [23]. To estimate the $W + \gamma$ background we use a matrix element generator [24] and use PYTHIA for the initial-state QCD radiation and hadronization. The background from W + jets, where a jet or track is misidentified as an electron or muon, is determined from the data. We first calculate the probability that a jet with a large fraction of its energy deposited in the electromagnetic calorimeter is misidentified as an electron, and the probability that a minimum ionizing track is misidentified as a muon. These probabilities are termed fake rates. The fake rate for each lepton type is calculated using an average of four inclusive jet samples (triggered with at least one jet with $E_T > 20$, 50, 70, or 100 GeV respectively). We remove sources of real leptons from Z decays using an

TABLE II: Summary of systematic uncertainties on the acceptance for each "signal" process. See text for further details.

Source	$t\bar{t}(ee)$	$t\bar{t}(e\mu)$	$t\bar{t}(\mu\mu)$	$W^+W^-(ee)$	$W^+W^-(e\mu)$	$W^+W^-(\mu\mu)$	$Z^0 \to \tau^+\tau^-$ $(e\mu)$
JES	5%	-	6%	1%	-	1%	-
ISR	8%	4%	6%	5%	5%	5%	5%
FSR	7%	3%	5%	-	-	-	-
Other	6%	5%	5%	5%	4%	4%	5%
Total	13%	7%	11%	7%	6%	7%	7%

invariant mass cut, and from W decays using a Monte Carlo estimate of the contamination, and parametrize the fake rates as a function of jet transverse energy for electrons, or track transverse momentum for muons. The background is determined by weighting the jets from a data sample of $(W \to \ell\nu) + \text{jets}$ events by the fake rates. As a result of very low statistics in the data for the calculation of the fake rates, and large uncertainties in other aspects of the calculation, we assume a 100% total uncertainty on our final $W + \text{jets}$ background estimates.

A summary of all expected contributions for each dilepton channel is given in Table III, together with observed numbers of events.

We extract the $t\bar{t}$, W^+W^-, and $Z^0 \to \tau^+\tau^-$ cross sections simultaneously for the $e\mu$ channel by maximizing the binned likelihood function:

$$L(\mu_{t\bar{t}}, \mu_{WW}, \mu_{\tau\tau}) = \prod_i^{N_{bin}} \frac{\mu_i^{n_i} e^{-\mu_i}}{n_i!} \times \prod_j G(x_j, \sigma_j) \quad (1)$$

where the index i runs over all N_{bin} bins in the two-dimensional $\not\!\!E_T - N_j$ parameter space, and j runs over all variables x_j, which are parameters in the likelihood function constrained by a Gaussian of width σ_j, the estimated uncertainty on x_j. These variables consist of the expected number of events for the background processes (given in Table III), the acceptances for the signal processes (given in Table I), and the integrated luminosity.

The parameters $\mu_{t\bar{t}}$, μ_{WW}, and $\mu_{\tau\tau}$ are the expected total numbers of $t\bar{t}$, W^+W^-, and $Z^0 \to \tau^+\tau^-$ events, respectively. The expected distributions of these processes in the $\not\!\!E_T - N_j$ parameter space determine the probabilities $p_{t\bar{t},i}$, $p_{WW,i}$, and $p_{\tau\tau,i}$ that a $t\bar{t}$, W^+W^-, or $Z^0 \to \tau^+\tau^-$ event, respectively, will appear in the i-th bin. Therefore, the total expected

TABLE III: The numbers of SM predicted events, and the numbers observed, in 360 pb^{-1} of data. For the $e\mu$ channel, where the only requirement is two high-p_T leptons, the first three processes are considered signals for which cross sections are measured. For the ee and $\mu\mu$ channels, where an additional $\not\!\!E_T^{sig}$ requirement is made, only the first two processes are regarded as signals. To calculate the expected number of events from our signal processes we used the cross section central values, $\sigma(t\bar{t}) = 6.1$ pb, $\sigma(W^+W^-) = 12.4$ pb, and $\sigma(Z^0 \to \tau^+\tau^-) = 251$ pb. Uncertainties on the theoretical cross sections are not included.

	$e\mu$	ee	$\mu\mu$	$\ell\ell$
$t\bar{t}$	10.0 ± 0.7	3.6 ± 0.5	3.4 ± 0.4	17.0 ± 1.6
W^+W^-	13.8 ± 0.8	5.2 ± 0.4	4.3 ± 0.3	23.3 ± 1.5
$Z^0 \to \tau^+\tau^-$	57.8 ± 4	1.1 ± 0.2	0.6 ± 0.1	59.5 ± 4.3
$DY \to ee$	0	15.4 ± 3.2	0	15.4 ± 3.2
$DY \to \mu\mu$	9.3 ± 0.8	0	11.6 ± 2.4	20.8 ± 3.2
WZ	0.70 ± 0.06	1.26 ± 0.09	1.11 ± 0.08	3.07 ± 0.23
ZZ	0.07 ± 0.01	0.47 ± 0.03	0.42 ± 0.03	0.96 ± 0.07
$W\gamma$	1.2 ± 0.5	1.8 ± 0.7	0	3.0 ± 1.2
$W +$ jets	3.0 ± 3.0	2.1 ± 2.1	1.6 ± 1.6	6.8 ± 6.8
Total SM	96 ± 5	31 ± 4	23 ± 3	150 ± 12
Data	103	24	29	156

number of events in the i-th bin of the $\not\!\!E_T - N_j$ parameter space is:

$$\mu_i = (p_{t\bar{t},i} \times \mu_{t\bar{t}}) + (p_{WW,i} \times \mu_{WW}) + (p_{\tau\tau,i} \times \mu_{\tau\tau}) + n_{other} \quad (2)$$

where n_{other} is the expected number of events in the i-th bin from all background processes, and is fixed in the likelihood fit within its Gaussian constraint. The product over i in the likelihood function is the product of Poisson probabilities for each bin, in which the expected number of events is μ_i, and n_i is the corresponding number of events observed in the data. We use 10 GeV wide bins for $\not\!\!E_T < 60$ GeV, and 20 GeV bins for $60 < \not\!\!E_T < 120$ GeV. Note that in Figs. 1 and 2 we show the $\not\!\!E_T - N_j$ shapes using a uniform 10 GeV binning in $\not\!\!E_T$.

For each of the signal processes, $\mu_k = \sigma_k \epsilon_k \mathcal{L}$, where $k = t\bar{t}$, W^+W^-, or $Z^0 \to \tau^+\tau^-$,

and σ_k is the production cross section for the process k, which is a free parameter in the likelihood fit. The acceptances, ϵ_k, and integrated luminosity of the data sample, $\mathcal{L}$, are fixed within a Gaussian constraint as mentioned above. By maximizing the likelihood function we extract the production cross sections for $t\bar{t}$, W^+W^-, and $Z^0 \to \tau^+\tau^-$.

We perform a similar likelihood fit to the full $ee + e\mu + \mu\mu$ data to extract $t\bar{t}$ and W^+W^- cross sections, in which we consider $Z^0 \to \tau^+\tau^-$ as a fixed background included in the n_{other} term, since in the ee and $\mu\mu$ channels it has been significantly reduced by the $\not\!\!E_T^{sig}$ requirement. We perform the full fit using a likelihood function that is the product of the individual likelihood functions for each channel. We also make the following assumptions about correlations in the full fit: within a given channel (ee, $e\mu$, or $\mu\mu$) we assume the signal acceptances are 100% correlated because they are driven by the lepton identification efficiencies, and between channels we assume no correlations in the acceptances. The latter is not actually true because, for example, the ee and $e\mu$ channels have correlations in the lepton identification uncertainties due to overlap in lepton types, and the ee and $\mu\mu$ channels share some JES systematic uncertainties. However, by varying these correlations between 0% and 100% we see a negligible effect on the extracted cross sections, so we use 0% for simplicity.

For both the $e\mu$-only and $ee + e\mu + \mu\mu$ scenarios we perform two sets of fits. Our main results are obtained by letting all the signal cross sections float, with the exception of $Z^0 \to \tau^+\tau^-$ in the ee and $\mu\mu$ channels, to simultaneously extract the signal cross sections from the fit. These results are summarized in Table IV, with the systematic uncertainties included in these results being discussed below. As a result of the good separation of our signal processes in the $\not\!\!E_T - N_j$ parameter space, we observe very little correlation between these cross section measurements. In the $e\mu$ channel fit where all three cross sections float, these correlations are about -0.06 between $\sigma(t\bar{t})$ and $\sigma(W^+W^-)$, -0.05 between $\sigma(t\bar{t})$ and $\sigma(Z^0 \to \tau^+\tau^-)$, and, -0.19 between $\sigma(W^+W^-)$ and $\sigma(Z^0 \to \tau^+\tau^-)$. The $t\bar{t}$ production cross section measurement is relatively insensitive to the top mass used for the $t\bar{t}$ acceptance in generating the $\not\!\!E_T - N_j$ template shape. We generated templates using a top mass of $178\,\mathrm{GeV}/c^2$ [25]. Using simulated experiments we observe a 1% variation in $\sigma(t\bar{t})$ if the top mass is varied between $165\,\mathrm{GeV}/c^2$ and $178\,\mathrm{GeV}/c^2$; therefore, we neglect any effects due to the uncertainty on the top mass.

Fits to the data are also performed by fixing all but one of the signal processes to their

SM expected values. We consider the results extracted from these fits as cross-checks, as they use the added constraint of assuming SM production for all processes other than the one being measured, in a similar fashion to the more standard counting experiment results. Significant differences between these cross-checks and our main results could be an indication that the SM assumptions being used are incorrect. We summarize the results from these fits in Table V. When fixed in a particular fit, we use the following SM theoretical predictions: $\sigma(t\bar{t}) = 6.1 \pm 0.9$ pb [26], $\sigma(W^+W^-) = 12.4 \pm 0.8$ pb [27], and $\sigma(Z^0 \to \tau^+\tau^-) = 251.3 \pm 5.0$ pb [28].

The uncertainties on the measured cross sections include a component coming from the fit (including statistical, acceptance systematic, and integrated luminosity) and a second one due to changes in the $\not\!\!E_T - N_j$ distributions caused by the systematic sources mentioned in Table II. The fit program used was MINUIT [29], which minimizes $-\ln(L)$, and determines the fit errors from the $-2\ln(L)$ values. To evaluate systematic changes in the shape of $\not\!\!E_T - N_j$ distributions, we use simulated experiments with one of the signal or background distributions from a Monte Carlo simulation with a particular systematic effect applied. The shape systematic uncertainties are summarized in Table VI.

TABLE IV: Cross section measurements from a global fit of 360 pb^{-1} of high-p_T dilepton data. The first uncertainty is the error returned by the likelihood fit, which includes statistical, acceptance systematic, and luminosity uncertainties. The magnitudes of the latter two uncertainties are given in Table II and in the text. The second is the systematic uncertainty in the template shapes.

Process	$e\mu$	$ee + \mu\mu + e\mu$
$\sigma(t\bar{t})$	$9.3^{+3.1\ +0.7}_{-2.6\ -0.2}$ pb	$8.5^{+2.6\ +0.7}_{-2.2\ -0.3}$ pb
$\sigma(W^+W^-)$	$11.4^{+5.2\ +0.5}_{-4.3\ -0.1}$ pb	$16.3^{+5.1\ +0.8}_{-4.4\ -0.2}$ pb
$\sigma(Z^0 \to \tau^+\tau^-)$	$291^{+50\ +6}_{-46\ -3}$ pb	-

In summary, we present a new method to study globally the production of events with final-states including two high-p_T leptons. We measure simultaneously the production cross sections for $t\bar{t}$, W^+W^-, and $Z^0 \to \tau^+\tau^-$ and obtain the following results: $\sigma(t\bar{t}) = 8.5^{+2.7}_{-2.2}$ pb, $\sigma(W^+W^-) = 16.3^{+5.2}_{-4.4}$ pb, and $\sigma(Z^0 \to \tau^+\tau^-) = 291^{+50}_{-46}$ pb. They are in good agreement with SM theoretical predictions. In addition to the potential this analysis technique has for precision cross section measurements in the dilepton channel with more data, it could also

TABLE V: Cross section measurements from a fit to the data with all but one signal process fixed to its SM value. See text for further details. The uncertainties have the same meaning as in Table IV.

Process	$e\mu$	$ee + \mu\mu + e\mu$
$\sigma(t\bar{t})$ (W^+W^-, $Z^0 \to \tau^+\tau^-$ fixed)	$9.3^{+3.1\ +0.7}_{-2.6\ -0.2}$ pb	$8.4^{+2.5\ +0.7}_{-2.1\ -0.3}$ pb
$\sigma(W^+W^-)$ ($t\bar{t}$, $Z^0 \to \tau^+\tau^-$ fixed)	$12.3^{+5.3\ +0.5}_{-4.4\ -0.1}$ pb	$16.1^{+5.0\ +0.8}_{-4.3\ -0.2}$ pb
$\sigma(Z \to \tau\tau)$ ($t\bar{t}$, W^+W^- fixed)	$293^{+49\ +6}_{-45\ -3}$ pb	-

TABLE VI: Summary of the shape systematic uncertainties for the $e\mu$ and full($ee + e\mu + \mu\mu$) fit.

Source	$t\bar{t}(e\mu)$	$W^+W^-(e\mu)$	$Z^0 \to \tau^+\tau^-(e\mu)$	$t\bar{t}$ (full)	W^+W^- (full)
JES	$^{+6}_{-1}\%$	$^{+4}_{-1}\%$	$^{+2}_{-1}\%$	$^{+7}_{-2}\%$	$^{+5}_{-1}\%$
ISR	$^{+4}_{-2}\%$	$\pm 1\%$	$\pm 1\%$	$^{+5}_{-2}\%$	$\pm 1\%$
FSR	$\pm 1\%$	—	—	$\pm 1\%$	—
Total	$^{+7}_{-2}\%$	$^{+4}_{-1}\%$	$^{+2}_{-1}\%$	$^{+8}_{-3}\%$	$^{+5}_{-1}\%$

be promising for model independent searches for new physics.

We thank the Fermilab staff and the technical staffs of the participating institutions for their vital contributions. This work was supported by the U.S. Department of Energy and National Science Foundation; the Italian Istituto Nazionale di Fisica Nucleare; the Ministry of Education, Culture, Sports, Science and Technology of Japan; the Natural Sciences and Engineering Research Council of Canada; the National Science Council of the Republic of China; the Swiss National Science Foundation; the A.P. Sloan Foundation; the Bundesministerium für Bildung und Forschung, Germany; the Korean Science and Engineering Foundation and the Korean Research Foundation; the Particle Physics and Astronomy Research Council and the Royal Society, UK; the Institut National de Physique Nucleaire et Physique des Particules/CNRS; the Russian Foundation for Basic Research; the Comisión Interministerial de Ciencia y Tecnología, Spain; the European Community's Human Poten-

tial Programme under contract HPRN-CT-2002-00292; and the Academy of Finland.

---

[1] F. Abe *et al.* (CDF Collaboration), Phys. Rev. Lett. **80**, 2779 (1998).

[2] R. M. Barnett and L. J. Hall, Phys. Rev. Lett. **77**, 3506 (1996).

[3] C. T. Hill, Phys. Lett. B **266**, 419 (1991).

[4] E. Arik *et al.*, Phys. Rev. D **66**, 033003 (2002).

[5] A. Abulencia *et al.* (CDF Collaboration), Phys. Rev. Lett. **97**, 081802 (2006).

[6] In the CDF coordinate system, θ and ϕ are the polar and azimuthal angles, respectively, with respect to the proton beam direction (z axis). The pseudorapidity η is defined as $-\ln\tan(\theta/2)$. The transverse momentum of a particle is $p_T = p\sin\theta$. The analogous quantity using calorimeter energies, defined as $E_T = E\sin\theta$, is called transverse energy.

[7] The missing transverse energy, $\vec{\not\!\!E}_T$, is defined as $-\sum E_T^i\,\hat{n}_i$, where $\hat{n}_i$ is the unit vector in the transverse plane pointing from the interaction point to the energy deposition in calorimeter cell i. The $\vec{\not\!\!E}_T$ measurement is corrected for muons in the event with $p_T > 20$ GeV/c, and for jet corrections. The magnitude of $\vec{\not\!\!E}_T$ is denoted as $\not\!\!E_T$.

[8] D. Acosta *et al.* (CDF Collaboration), Phys. Rev. Lett. **93**, 142001 (2004).

[9] D. Acosta *et al.* (CDF Collaboration), Phys. Rev. Lett. **94**, 211801 (2005).

[10] A. Safonov, Nucl. Phys. Proc. Suppl. **144**, 323-332 (2005).

[11] D. Acosta *et al.* (CDF Collaboration), Phys. Rev. D **71**, 032001 (2005).

[12] G. C. Blazey and B. L. Flaugher, Ann. Rev. of Nucl. and Part. Sci. Vol. **49** (1999).

[13] A. Bhatti *et al.*, Nucl. Instrum. Methods A **566**, 375 (2006).

[14] A. Abulencia *et al.*(CDF Collaboration), hep-ex/0508029, submitted to Phys. Rev. D.

[15] The calorimeter isolation I_{cal} is defined as the extra energy deposited in the calorimeter cone of radius $\Delta R = \sqrt{\Delta\phi^2 + \Delta\eta^2} = 0.4$ around the lepton. The I_{cal} is required to be less than 10 % of the lepton E_T.

[16] The track isolation I_{trk} is defined as the sum of the p_T of all the tracks in a cone of radius $\Delta R = \sqrt{\Delta\phi^2 + \Delta\eta^2} = 0.4$ around the lepton candidate track, but excluding it. The I_{trk} is required to be less than 10% of the lepton track p_T.

[17] T. Sjöstrand *et al.*, Comput. Phys. Commun. **135**, 238 (2001). We use PYTHIA V6.2.

[18] R. Brun and F. Carminati, CERN Program Library Long Writeup W5013, 1993 (unpublished).

[19] We compared the acceptances obtained using MRST 72 and 75 PDF sets [20], corresponding to $\alpha_s = 0.1175$ and 0.1125 respectively. Also we include the effect of the eigenvector variations around the fit minima, using CTEQ6M PDF sets [21], and used the maximum variation observed in the acceptance as our systematic uncertainty.

[20] A. D. Martin, R. G. Roberts, W. J. Stirling, and R. S. Thorne, hep-ph/0307262.

[21] H. L. Lai *et al.*, Phys. Rev. D **51**, (1995).

[22] S. Klimenko, J. Konigsberg, and T.M. Liss, FERMILAB-FN-0741 (2003).

[23] J. M. Campbell and R. K. Ellis, Phys. Rev. D **60**, 113006 (1999).

[24] U. Baur and E. L. Berger, Phys. Rev. D **41**, 1476 (1990); U. Baur and E. L. Berger, Phys. Rev. D **47**, 4889 (1993).

[25] P. Azzi *et al.* (for the CDF and DØ collaborations), hep-ex/0404010; superseded by hep-ex/0608032.

[26] R. Bonciani, S. Catani, M. L. Mangano, and P. Nason, Nucl. Phys. B **529**, 424 (1998), update in hep-ph/0303085.

[27] J. M. Campbell and R. K. Ellis, Phys. Rev. D **60** (1999) 113006; next-to-leading-order calculation using MCFM version 3.4.5.

[28] A. D. Martin, R. G. Roberts, W. J. Stirling, and R. S. Thorne, Eur. Phys. J. C **35**, 325-348 (2004).

[29] F. James, CERN Program Library Long Writeup D506, MINUIT reference manual version 94.1, 1998 (unpublished).